Original Article

Detecting lymph node metastasis of esophageal cancer on dual-energy computed tomography

Acta Radiologica
2022, Vol. 63(1) 3–10

DOI: 10.1177/0284185120980144
journals.sagepub.com/home/acr

Xuyang Sun[1], Tetsu Niwa[1], Soji Ozawa[2], Jun Endo[1] and Jun Hashimoto[1]

Abstract

Background: Using conventional computed tomography (CT), the accurate diagnosis of lymph node (LN) metastasis of esophageal cancer is difficult.

Purpose: To examine dual-energy CT parameters to predict LN metastasis preoperatively in patients with esophageal cancer.

Material and Methods: Twenty-six consecutive patients who underwent dual-energy CT before an esophageal cancer surgery (19 patients with LN metastases) were analyzed. The included LNs had a short-axis diameter of $\geq$4 mm and were confirmed to be resected on postoperative CT. Their short-axis diameter, CT value, iodine concentration (IC), and fat fraction were measured on early- and late-phase contrast-enhanced dual-energy CT images and compared between pathologically confirmed metastatic and non-metastatic LNs.

Results: In total, 51 LNs (34 metastatic and 17 non-metastatic) were included. In the early phase, IC and fat fraction were significantly lower in the metastatic than in the non-metastatic LNs (IC = 1.6 mg/mL vs. 2.2 mg/mL; fat fraction = 20.3% vs. 32.5%; both $P < 0.05$). Furthermore, in the late phase, IC and fat fraction were significantly lower in the metastatic than in the non-metastatic LNs (IC = 2.0 mg/mL vs. 3.0 mg/mL; fat fraction = 20.4% vs. 33.0%; both $P < 0.05$). Fat fraction exhibited accuracies of 82.4% and 78.4% on early- and late-phase images, respectively. Conversely, short-axis diameter and CT value on both early- and late-phase images were not significantly different between the metastatic and non-metastatic LNs ($P > 0.05$).

Conclusion: Using dual-energy CT images, IC and fat fraction are useful for diagnosing LN metastasis in patients with esophageal cancer.

Keywords
Esophageal cancer, lymph node metastasis, dual-energy computed tomography, iodine concentration, fat fraction

Date received: 19 August 2020; accepted: 17 November 2020

Introduction

Esophageal cancer is one of the most common malignancies of the digestive system and is the sixth leading cause of death and the eighth most common cancer worldwide (1,2). The five-year survival rate of patients with esophageal cancer is approximately 15%–25% (1–3). The most common histological type of esophageal cancer is squamous cell carcinoma in Asia and adenocarcinoma in Europe and the United States (1), with other types being rare (4). Esophageal cancer is associated with a very low survival rate because most patients have advanced disease upon diagnosis (1). The radiological staging of esophageal cancer is complex but essential for clinical treatment. Accurate staging should be performed to guide treatment decisions and determine patient prognosis.

[1]Department of Diagnostic Radiology, Tokai University School of Medicine, Isehara, Japan
[2]Department of Gastroenterological Surgery, Tokai University School of Medicine, Isehara, Japan

Corresponding author:
Tetsu Niwa, Department of Radiology, Tokai University School of Medicine, 143 Shimokasuya, Isehara, 259-1193, Japan.
Email: niwat@tokai-u.jp

Lymph node (LN) metastases due to esophageal cancer occur in the neck as well as the mediastinal and abdominal areas. The incidence of LN metastases of esophageal cancer is higher than those of LN metastases of other gastrointestinal cancers (5). LN metastasis has been considered an important factor influencing the prognosis of esophageal cancer (6,7). In a study reporting patient survival on the basis of the number of LN metastases, the five-year survival rate after esophagectomy was 68.2% in patients without LN metastases, 46.4% in those with 1–3 LN metastases, and 25.2% in those with 4–7 LN metastases (5). Although 11.2% of patients with esophageal cancer have >8 LN metastases (5), accurate clinical diagnosis of LN metastasis remains difficult (6). Currently, computed tomography (CT) is the most commonly used method to assess primary tumor, metastases, and LN status in patients with esophageal cancer (8). LN metastasis is generally assessed based on LN enlargement. However, this imaging finding is not sufficiently sensitive or specific (6,9). Other findings such as the shape and CT attenuation of LNs have also been used, albeit without high accuracy (10). Characterizing LNs as being metastatic or not is difficult using conventional CT (6,9,11,12) in patients with esophageal cancer due to the presence of several LN micrometastases in them (5).

However, LNs may be further characterized using dual-energy CT (13–17). Dual-energy CT uses data from two different X-ray spectra, typically with low energy of 80 kVp and high energy of 140–150 kVp (18). Various types of images can be obtained through data processing using dual-energy CT, such as mixed energy images, iodine maps, virtual non-contrast images, and monoenergetic images (12,13,19).

Studies have reported the role of dual-energy CT in assessing LN metastasis of neck and abdominal cancers (20–24). In the present study, we introduced material characterization and degradation functions and hypothesized that dual-energy CT improves the diagnostic accuracy of differentiating metastatic from non-metastatic LNs in patient with esophageal cancer. Therefore, the aim of the present study was to assess the ability of dual-energy CT to detect LN metastasis in patients with esophageal cancer.

Material and Methods

Participants

In total, 74 consecutive patients with esophageal cancer underwent dual-energy CT as an initial evaluation from February 2017 to February 2018. The images were retrospectively reviewed. First, patients who did not undergo esophagectomy were excluded (n = 32). Next, all CT images were reviewed by two radiologists with 22 and 26 years of experience; LNs with a short-axis diameter of > 4 mm were noted. These LNs were referred on postoperative CT images and confirmed as "resected" or "non-resected"; patients without recognizable resected LNs were also excluded (n = 16). Finally, patients with identifiable LNs with a short-axis diameter of > 4 mm preoperatively, which were postoperatively confirmed as "resected," were included (n = 26, 22 men, 4 women; mean age. 69.7 years; age range. 42–82 years) (Fig. 1). The present study was approved by out institutional review board. Informed consent was waived due to the retrospective nature of the study.

The patients' tumor stages were assessed using the 8th edition of the Union for International Cancer Control TNM staging: 0 (n = 2); I (n = 5); II (n = 3); III (n = 11); and IV (n = 5) (25). Ten patients underwent preoperative neoadjuvant chemotherapy (cisplatin and 5-fluorouracil [n = 5]; docetaxel, cisplatin, and 5-fluorouracil [n = 5]) and three underwent preoperative chemoradiotherapy (total dose = 41.4 Gy; cisplatin and 5-fluorouracil). Of the patients, 19 (73.1%) had metastatic LNs and 7 (26.9%) had non-metastatic LNs. The histological type of metastatic tumor was squamous cell carcinoma in 23 (88.5%) patients, adenocarcinoma in 2 (7.7%) patients, and adenoneuroendocrine carcinoma in 1 (3.8%) patient. The number of identified LNs in each patient was 1–5 (mean = 2.0). A total of 51 LNs (pathologically confirmed 34 metastatic and 17 non-metastatic) were analyzed in the 26 patients.

CT examination

CT was performed using a dual-energy scanner (SOMATOM Force, Siemens Healthcare, Forchheim, Germany). For performing contrast-enhanced CT, contrast material containing 300 mg of iohexol/mL (Omnipaque, GE Healthcare, Chicago, IL, USA) was injected using an injector at a rate of 23 mg I/kg/s for 20 s through an 18-G needle at the antecubital vein. Early-phase images were acquired at the timing determined using a bolus tracking method; when the CT value in the ascending aorta reached 180 HU, the early phase was started. The included scan area was from the top of the chest to the diaphragm in the early phase and from the neck to the pelvis in the late phase. The dual-energy scan settings were as follows: tube voltages = 90 and 150 kVp; gantry rotation time = 0.25 s; pitch = 0.55; 192 × 0.6 mm; and automatic current modulation (CARE Dose 4D). Patients were instructed to hold their breath before obtaining CT scans. Electrocardiogram gating was not used. Scan data were reconstructed in a field of view of 350 mm

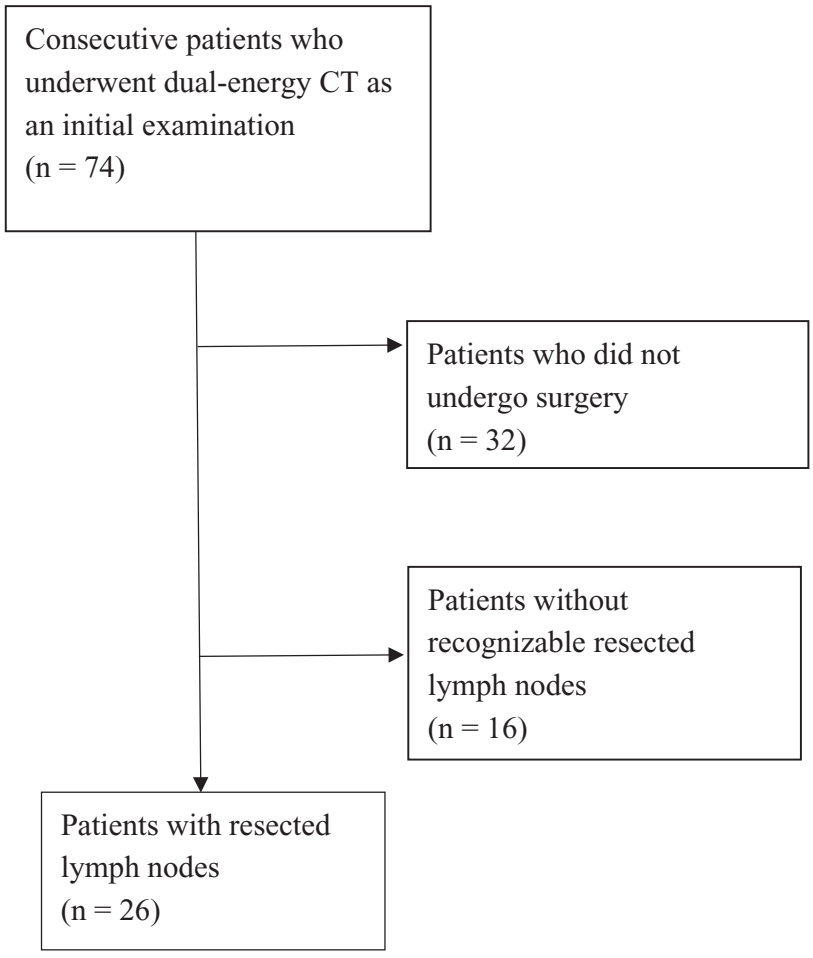

Fig. 1. Flow diagram of patient inclusion and exclusion criteria.

and matrix of 512 × 512 using a soft-tissue convolution kernel of Bf40 with a slice thickness of 1 mm and increments of 0.8 mm.

Image analysis

CT images were transferred to a workstation (Syngo. via VB20A, Siemens Healthcare, Forchheim, Germany), after which image analysis was performed. First, iodine maps were created on the workstation to calculate iodine concentration (IC) and fat fraction using iodine subtraction algorithm (Liver VNC, Siemens). Next, rounded regions of interest (ROIs) were manually drawn on the longest axis of the LNs by a radiologist with 22 years of experience in chest imaging. The short-axis diameter, CT value, IC, and fat fraction in each LN were measured on the workstation (Fig. 2). CT value was determined by blending 60% of CT values at low keV and 40% of CT values at high keV. Simultaneously, an ROI was placed on the descending aorta at the tracheal bifurcation level and IC in the descending aorta was recorded. IC was corrected for the aortic IC defined as normalized IC using the following citation:

$$\text{Normalized IC} = \text{IC}_{\text{LN}}/\text{IC}_{\text{aorta}}$$

where IC_{LN} and IC_{aorta} are ICs for LNs and the aorta, respectively.

These measurements were repeated one month later by the same observer who was blinded to previous measurements, and the values for each measurement were averaged.

Statistical analysis

LN metastasis was determined via postoperative pathological examination. The surgeons marked the number of resected LNs according to the location described in the Japanese Classification of Esophageal Cancer, 11th edition (26,27). The resected LNs were correlated with those on CT using these numbers. The measured parameters comprising short-axis diameter, CT value, IC, normalized IC, and fat

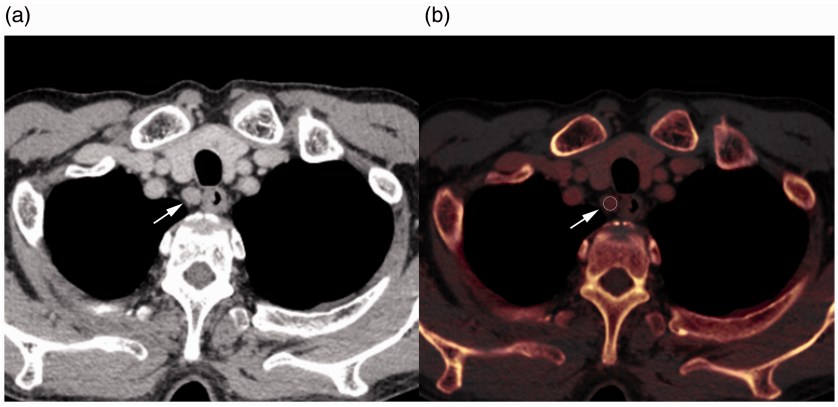

Fig. 2. Contrast-enhanced CT image (a) and iodine map (b) of a 69-year-old man with esophageal cancer. Regions of interest (b, circle) were placed at the center of the right cervical para-esophageal lymph nodes (a and b, arrow). The short-axis diameter, CT value, iodine concentration, and fat fraction were measured. CT, computed tomography.

Table 1. Comparison of dual-energy CT parameters between metastatic and non-metastatic lymph nodes.

Parameters	Metastatic lymph nodes (n = 34)	Non-metastatic lymph nodes (n = 17)	*P* value
Short-axis diameter (mm)	7.5 (4.8–10.0)	5.9 (5.3–6.6)	0.121
Early phase			
CT value (HU)	71.4 (62.6–86.8)	79.4 (57.0–84.6)	1.000
Iodine concentration (mg/mL)	1.60 (1.15–2.10)	2.20 (1.88–2.67)	0.003
Normalized iodine concentration	0.113 (0.075–0.132)	0.131 (0.107–0.169)	0.017
Fat fraction (%)	19.4 (15.9–23.9)	29.1 (24.8–38.5)	0.0001
Late phase			
CT value (HU)	74.2 (63.1–86.0)	76.3 (66.7–85.7)	0.646
Iodine concentration (mg/mL)	1.98 (1.50–2.40)	2.90 (2.50–3.29)	0.0002
Normalized iodine concentration	0.536 (0.402–0.672)	0.795 (0.639–0.881)	0.0002
Fat fraction (%)	17.0 (14.7–24.5)	34.0 (26.1–39.8)	0.0001

Data are presented as median (IQR).
CT, computed tomography; IQR, interquartile range.

fraction of LNs on the early- and late-phase images were compared between the metastatic and non-metastatic LNs using the Mann–Whitney test. Then, receiver operating characteristic (ROC) curves were assessed for parameters showing significant differences between the metastatic and non-metastatic LNs; cut-off values, sensitivity, specificity, accuracy, and area under the ROC curve (AUC) were determined. AUC was interpreted as follows: 0.7–0.8 = acceptable; 0.8–0.9 = excellent and >0.9 = outstanding (28). The cut-off value was defined by the point on the ROC curve with the minimum distance from 0% false-positive rate and 100% true-positive rate. Intra-rater agreements were assessed using the intra-class correlation (ICC); ICCs were interpreted as follows: 0.01–0.20 = slight agreement; 0.21–0.40 = fair agreement; 0.41–0.60 = moderate agreement; 0.61–0.80 = substantial agreement; and 0.81–1.0 = near-perfect agreement (29). Statistical analysis was performed using MedCalc Statistical Software version 19.2 (MedCalc Software Ltd, Ostend, Belgium). ROC analysis was performed using EZR statistical analysis software version 1.42 (Saitama Medical Center, Jichi Medical University, Saitama, Japan) (30). Descriptive values were presented as median (interquartile range).

Results

Dual-source CT analysis

Table 1 shows the results of comparisons of the assessed factors between the metastatic and non-metastatic LNs. Short-axis diameters showed a trend toward greater diameter in the metastatic LNs; however, these did not significantly differ between the metastatic (7.5 mm [range = 4.8–10.0 mm]) and non-metastatic (5.9 mm [range = 5.3–6.6 mm]) LNs ($P = 0.121$).

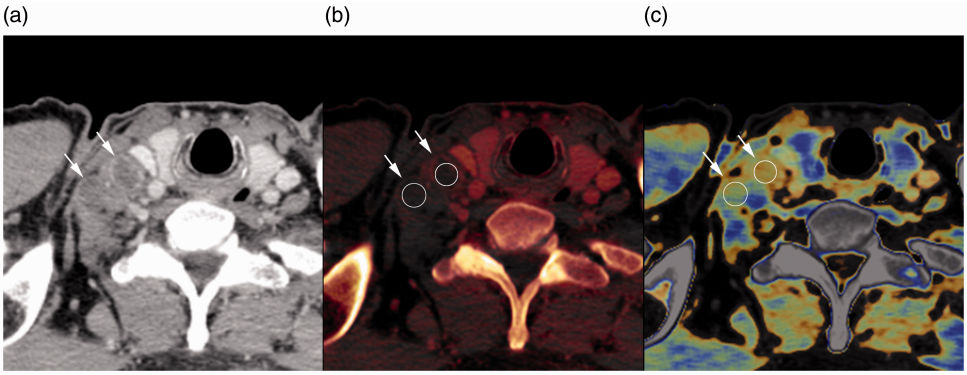

Fig. 3. Contrast-enhanced CT image (a), iodine map (b), and fat map (c) of a 55-year-old man with esophageal cancer in the late phase. Regions of interest (b and c, circle) were placed at the center of the two right supraclavicular lymph nodes (a–c, arrows). Iodine concentration values were 0.25 mg/mL and 0.20 mg/mL, and fat fraction values were 17.0% and 17.6% for each lymph node, respectively. Iodine concentration and fat fraction were significantly lower in metastatic lymph nodes than in non-metastatic lymph nodes.

In the early phase, CT values did not significantly differ between the metastatic and non-metastatic LNs (71.4 HU [range = 62.6–86.8 HU] vs. 79.4 HU [range = 57.0–84.6 HU]; $P = 1.000$). ICs were significantly lower in the metastatic LNs than in the non-metastatic LNs (1.60 mg/mL [range = 1.15–2.10 mg/mL] vs. 2.20 mg/mL [range = 1.88–2.67 mg/mL]; $P = 0.003$). Furthermore, normalized ICs were significantly lower in the former than in the latter (0.113 [range = 0.075–0.132] vs. 0.131 [range = 0.107–0.169]; $P = 0.017$). Fat fractions were also significantly lower in the metastatic LNs than in the non-metastatic LNs (19.4% [range = 15.9%–23.9%] vs. 29.1% [range = 24.8%–38.5%]; $P = 0.0001$).

In the late phase, CT values did not significantly differ between the metastatic and non-metastatic LNs (74.2 HU [range = 63.1–86.0 HU] vs. 76.3 HU [range = 66.7–85.7 HU]; $P = 0.646$). ICs were significantly lower in the metastatic LNs than in the non-metastatic LNs (1.98 mg/mL [range = 1.50–2.40 mg/mL] vs. 2.90 mg/mL [range = 2.50–3.29 mg/mL]; $P = 0.0002$). Furthermore, normalized ICs were significantly lower in the former than in the later (0.536 [0.402–0.672] vs. 0.795 [0.639–0.881]; $P = 0.0002$). Fat fractions were also significantly lower in the metastatic LNs than in the non-metastatic LNs (17.0% [14.7%–24.5%] vs. 34.0% [26.1%–39.8%]; $P = 0.0001$).

IC, normalized IC, and fat fractions were significantly different between the metastatic and non-metastatic LNs on both early- and late-phase images (Fig. 3), as assessed for ROC analysis. Table 2 shows the results of ROC analysis with the cut-off value, sensitivity, specificity, accuracy, and AUC for detecting metastatic LNs. AUCs for IC (0.755) and normalized IC (0.706) on early-phase images were acceptable. AUCs for fat fraction (0.848) on early-phase images and those for IC (0.827), normalized IC (0.822), and fat fraction (0.843) on late-phase images were excellent. The highest AUC was achieved for fat fraction on early-phase images, followed by that on late-phase images. Sensitivity, specificity, and accuracy for fat fraction were 73.5%, 88.2%, and 82.4% on early-phase and 79.4%, 76.5%, and 78.4% on late-phase images, respectively.

Intra-rater agreements were observed to be near-perfect as shown by ICCs of 0.962–0.976.

Discussion

We found that the metastatic and non-metastatic LNs in the patients with esophageal cancer exhibited significant differences regarding parameters such as IC, normalized IC, and fat fraction on both early- and late-phase images. These parameters can be considered to have diagnostic value in identifying metastatic LNs in patients with esophageal cancer.

In the present study, IC and normalized IC were significantly lower in the metastatic LNs than in the non-metastatic LNs on both early- and late-phase images. Dual-energy CT quantitatively estimates IC, which may reflect the vascularity or perfusion in LNs (15). Low IC in metastatic LNs may reflect hypovascularity in them. Previous studies reported that metastatic LNs in patients with colorectal, gynecological, and lung cancers had low IC or normalized IC on dual-energy CT images (15,21,22). In addition, a histological study (31) showed that vessel density was lower in metastatic LNs than in non-metastatic LNs in patients with neck cancer. Considering these reports, a similar situation is suggested in metastatic LNs in patients with esophageal cancer. In addition, some metastatic LNs might have necrosis, which may also result in low ICs. Conversely, metastatic LNs reportedly had higher IC

Table 2. Receiver operating characteristics for measured data with area under the receiver operating characteristic curve (AUC).

Parameters	Cut-off	Sensitivity (%)	Specificity (%)	Accuracy (%)	AUC (95% CI)
Early phase					
Iodine concentration (mg/mL)	1.85	67.8	76.4	70.6	0.755 (0.614–0.846)
Normalized iodine concentration	0.151	94.1	47.1	78.4	0.706 (0.549–0.863)
Fat fraction (%)	22.7	73.5	88.2	82.4	0.848 (0.730–0.966)
Late phase					
Iodine concentration (mg/mL)	2.40	79.4	82.4	72.5	0.827 (0.702–0.952)
Normalized iodine concentration	0.612	70.6	82.4	74.5	0.822 (0.701–0.942)
Fat fraction (%)	25.3	79.4	76.5	78.4	0.843 (0.736–0.950)

AUC, area under the receiver operating characteristic curve; CI, confidence interval.

and normalized IC than non-metastatic LNs in patients with hepatocellular carcinoma (20) and papillary thyroid cancer (32). Therefore, vascularity in metastatic LNs may vary depending on the origin of cancers.

IC may be influenced by the method of the contrast material injection. Therefore, in the present study, ICs were normalized using the IC of the aorta. The predictability for LN metastasis did not differ between IC and normalized IC. As the contrast agent was administered according to each patient's body weight, normalization might not have been needed in our contrast injection model.

CT values did not differ between the metastatic and non-metastatic LNs in this study. Although CT values on contrast-enhanced CT images may reflect vascularity to some extent, they may not directly reflect the amount of enhancement; furthermore, CT values on contrast-enhanced CT images would be affected by baseline CT values without contrast materials. A previous study (17) assessing CT values in abdominal LNs also showed an overlap between metastatic and non-metastatic LNs. Thus, CT value may not be useful to characterize LN metastasis of esophageal cancer. Conversely, iodine map is generated using the method based on three-material decomposition algorithms (14). ICs are estimated as the amount of contrast enhancement, which might reflect the tissue blood volume and vessel permeability (24) and help characterize metastatic LNs.

Fat fractions were significantly lower in the metastatic LNs than in the non-metastatic LNs in this study. A normal LN is known to have a relatively large fatty hilum, which may be observed on ultrasonography or CT images (33,34); the absence of this finding suggests LN metastasis. Miao et al. (35) analyzed CT findings of metastatic LNs in patients with colorectal cancer and reported that LNs with a middle fat depression forming a kidney bean shape were non-metastatic, whereas morphological changes were observed in metastatic LNs. A similar situation is suggested for metastatic LNs in patients with esophageal cancer. When LNs are infiltrated by tumor cells, the fat proportion decreases, resulting in low fat fraction on dual-energy CT images. Observation of the hilum fat on CT images may be difficult in case of small LNs. In such cases, fat fraction should be assessed using dual-energy CT. In this study, fat fraction was found to be a relatively good predictor of LN metastasis.

Conventionally, LN metastasis of esophageal cancer has been assessed according to size. LN metastasis has been clinically considered as having a short-axis diameter of $\geq$8–10 mm (9,17,36,37). Similar criteria are also generally used in other types of cancer. Reportedly, CT can identify enlarged LNs, leading to suspected tumour involvement (38). However, the LN size criteria result in a relatively poor diagnostic accuracy because metastasis is reported in some LNs with small diameter (2,6,11). Foley et al. (9) reported that sensitivity, specificity and accuracy for LN metastasis according to the size criteria on CT images were 39.7%, 77.3% and 54.5%, respectively. In this study, the maximum short-axis diameters of metastatic LNs showed a trend toward greater diameters than those of non-metastatic LNs. However, similar to the previous study (9), metastatic and non-metastatic LNs could not be differentiated according to size alone in our patients and an overlap was observed. While enlarged LNs are metastatic, non-enlarged LNs have the possibility of being metastatic. In such relatively small LNs, dual-energy CT may be useful for additional characterisation.

The present study has several limitations. The study sample was relatively small. Only operated patients were included in this study; therefore, analyzed LN numbers were relatively small. Furthermore, LNs with a short-axis diameter of $>$4 mm were analyzed, leading to exclusion of metastatic LNs with a short-axis diameter of $\leq$4 mm. LNs on CT images were correlated with the resected LNs according to the LN number. Some patients underwent chemotherapy or chemoradiotherapy after the initial CT, which might have affected the results. In addition, histologically

different types of tumors were observed in the metastatic LNs, which might also have influenced our results. Although fat fraction on dual-energy CT may be a relatively good predictor compared with the method using conventional CT, there is still room for improvement for the detectability of LN metastases. Thus, further characterization of LN metastasis may be required.

In conclusion, IC and fat fraction on dual-energy CT images are useful for diagnosing LN metastasis in preoperative patients with esophageal cancer. Compared with the conventional CT, dual-energy CT may improve the diagnostic value for LN metastasis.

Declaration of conflicting interests

The author(s) declared no potential conflicts of interest with respect to the research, authorship, and/or publication of this article.

Funding

The author(s) received no financial support for the research, authorship, and/or publication of this article.

ORCID iD

Tetsu Niwa https://orcid.org/0000-0003-2861-0057

References

1. Domper Arnal MJ, Ferrandez Arenas A, Lanas Arbeloa A. Esophageal cancer: risk factors, screening and endoscopic treatment in Western and Eastern countries. World J Gastroenterol 2015;21:7933–7943.
2. Mehta K, Bianco V, Awais O, et al. Minimally invasive staging of esophageal cancer. Ann Cardiothorac Surg 2017;6:110–118.
3. Spataro J, Zfass AM, Schubert M, et al. Early esophageal cancer: a gastroenterologist's disease. Dig Dis Sci 2019;64:3048–3058.
4. Huang FL, Yu SJ. Esophageal cancer: risk factors, genetic association, and treatment. Asian J Surg 2018;41:210–215.
5. Akutsu Y, Matsubara H. Lymph node dissection for esophageal cancer. Gen Thorac Cardiovasc Surg 2013;61:397–401.
6. Foley K, Findlay J, Goh V. Novel imaging techniques in staging oesophageal cancer. Best Pract Res Clin Gastroenterol 2018;36-37:17–25.
7. Shang QX, Yang YS, Hu WP, et al. Prognostic significance and role of thoracic lymph node metastasis based on Chinese expert consensus in esophageal cancer. Ann Transl Med 2019;7:381.
8. Wang ZL, Zhou ZG, Chen Y, et al. Support vector machines model of computed tomography for assessing lymph node metastasis in esophageal cancer with neoadjuvant chemotherapy. J Comput Assist Tomogr 2017;41:455–460.
9. Foley KG, Christian A, Fielding P, et al. Accuracy of contemporary oesophageal cancer lymph node staging with radiological-pathological correlation. Clin Radiol 2017;72:693.e1–693.e7.
10. Wakita A, Motoyama S, Sato Y, et al. Evaluation of metastatic lymph nodes in cN0 thoracic esophageal cancer patients with inconsistent pathological lymph node diagnosis. World J Surg Oncol 2020;18:111.
11. van Rossum PSN, van Lier A, Lips IM, et al. Imaging of oesophageal cancer with FDG-PET/CT and MRI. Clin Radiol 2015;70:81–95.
12. Tawfik AM, Razek AA, Kerl JM, et al. Comparison of dual-energy CT-derived iodine content and iodine overlay of normal, inflammatory and metastatic squamous cell carcinoma cervical lymph nodes. Eur Radiol 2014;24:574–580.
13. Goo HW, Goo JM. Dual-energy CT: new horizon in medical imaging. Korean J Radiol 2017;18:555–569.
14. Naruto N, Itoh T, Noguchi K. Dual energy computed tomography for the head. Jpn J Radiol 2018;36:69–80.
15. Megibow AJ, Kambadakone A, Ananthakrishnan L. Dual-energy computed tomography: image acquisition, processing, and workflow. Radiol Clin North Am 2018;56:507–520.
16. D'Angelo T, Cicero G, Mazziotti S, et al. Dual energy computed tomography virtual monoenergetic imaging: technique and clinical applications. Br J Radiol 2019;92:20180546.
17. Martin SS, Czwikla R, Wichmann JL, et al. Dual-energy CT-based iodine quantification to differentiate abdominal malignant lymphoma from lymph node metastasis. Eur J Radiol 2018;105:255–260.
18. Nair JR, Burrows C, Jerome S, et al. Dual energy CT: a step ahead in brain and spine imaging. Br J Radiol 2020;93:20190872.
19. Taylor RE, Mager P, Yu NC, et al. Iodine quantification and detectability thresholds among major dual-energy CT platforms. Br J Radiol 2019;92:20190530.
20. Zeng YR, Yang QH, Liu QY, et al. Dual energy computed tomography for detection of metastatic lymph nodes in patients with hepatocellular carcinoma. World J Gastroenterol 2019;25:1986–1996.
21. Rizzo S, Radice D, Femia M, et al. Metastatic and non-metastatic lymph nodes: quantification and different distribution of iodine uptake assessed by dual-energy CT. Eur Radiol 2018;28:760–769.
22. Sato K, Morohashi H, Tsushima F, et al. Dual energy CT is useful for the prediction of mesenteric and lateral pelvic lymph node metastasis in rectal cancer. Mol Clin Oncol 2019;10:625–630.
23. Zhou Z, Liu Y, Meng K, et al. Application of spectral CT imaging in evaluating lymph node metastasis in patients with gastric cancers: initial findings. Acta Radiol 2019;60:415–424.
24. Yang Z, Zhang X, Fang M, et al. Preoperative diagnosis of regional lymph node metastasis of colorectal cancer with quantitative parameters from dual-energy CT. AJR Am J Roentgenol 2019;213:W17–W25.

25. Brierley JD, Gospodarowicz MK, Wittekind C (eds). TNM classification of malignant tumors. 8th ed. Oxford: Wiley-Blackwell, 2017.
26. Japan Esophageal Society. Japanese classification of esophageal cancer, 11th edition: part I. Esophagus 2017;14:1–36.
27. Japan Esophageal Society. Japanese classification of esophageal cancer, 11th edition: part II and III. Esophagus 2017;14:37–65.
28. Mandrekar JN. Receiver operating characteristic curve in diagnostic test assessment. J Thorac Oncol 2010;5:1315–1316.
29. Landis JR, Koch GG. The measurement of observer agreement for categorical data. Biometrics 1977;33:159–174.
30. Kanda Y. Investigation of the freely available easy-to-use software 'EZR' for medical statistics. Bone Marrow Transplant 2013;48:452–458.
31. Naresh KN, Nerurkar AY, Borges AM. Angiogenesis is redundant for tumour growth in lymph node metastases. Histopathology 2001;38:466–470.
32. He M, Lin C, Yin L, et al. Value of dual-energy computed tomography for diagnosing cervical lymph node metastasis in patients with papillary thyroid cancer. J Comput Assist Tomogr 2019;43:970–975.
33. Ewing DE, Layfield LJ, Joshi CL, et al. Determinants of false-negative fine-needle aspirates of axillary lymph nodes in women with breast cancer: Lymph node size, cortical thickness and hilar fat retention. Acta Cytol 2015;59:311–314.
34. Abe H, Schmidt RA, Sennett CA, et al. US-guided core needle biopsy of axillary lymph nodes in patients with breast cancer: why and how to do it. Radiographics 2007;27 Suppl 1:S91–99.
35. Miao SS, Lu YF, Chen HY, et al. Contrast-enhanced CT imaging for the assessment of lymph node status in patients with colorectal cancer. Oncol Lett 2020;19:3451–3458.
36. Lee HN, Kim JI, Shin SY, et al. Combined CT texture analysis and nodal axial ratio for detection of nodal metastasis in esophageal cancer. Br J Radiol 2020;93:20190827.
37. Sugawara K, Yamashita H, Uemura Y, et al. Preoperative lymph node status on computed tomography influences the survival of pT1b, T2 and T3 esophageal squamous cell carcinoma. Surg Today 2019;49:378–386.
38. Krasna MJ. Minimally invasive staging for esophageal cancer. Chest 1997;112:191S–194S.